Ground-State, Excited-Singlet-State, and Excited-Triplet-State Energy Levels and Photophysics of the Three Rotational Isomers of Isophthalaldehyde Vapor

Takao Itoh*

Graduate School of Integrated Arts and Sciences, Hiroshima University, 1-7-1 Kagamiyama, Higashi-Hiroshima City 739-8521, Japan

Emission, excitation, and absorption spectra of isophthalaldehyde (benzene-1,3-dicarboxaldehyde) vapor have been measured at different temperatures, along with the UV−vis and IR absorption spectra in solution. Analyses of the temperature dependence of the phosphorescence and excitation spectra of isophthalaldehyde vapor revealed the energetic relationships among the three rotational isomers in the $T_1(n, \pi^*)$, $S_1(n, \pi^*)$, and ground states. This appears to be the first example of the system where the S_0, T_1, and S_1 energy levels are determined for the three rotational isomers. The phosphorescence, fluorescence, and excitation origins of the three rotamers were assigned on the basis of the results of the density functional theory (DFT) and semiempirical SCF-MO calculations and infrared data as well as on the basis of the temperature dependence of the emission and excitation spectra.

1. Introduction

Rotational isomers (rotamers) exist for a number of molecules possessing the rotatable groups in general. However, it is not easy to identify the rotamers spectroscopically and to investigate the dynamical behavior of each rotamer in both the ground and excited states, because normally the electronic energy levels of the rotamers are located very close to one another.[1] Three planar and stable rotamers are considered to exist for isophthalaldehyde (benzene-1,3-dicarboxaldehyde, hereafter referred to as IP), as illustrated in Figure 1. The evidence for the existence of the three rotamers has not been provided so far for this molecule, although the presence of the two rotamers has been indicated by NMR.[2−4] Infrared spectral data also have been reported,[5−7] but the infrared spectroscopy has not provided any evidence for the existence of the three rotamers. Further, the detailed analyses of the vapor-phase emission spectrum are not available in the literature. Because the molecules in the vapor phase suffer no interaction from the environment, some molecules exhibit comparatively sharp emission bands in the static-vapor phase, as have been reported for benzaldehyde and its derivatives.[8−10] The static-vapor experiments can provide information on the temperature dependence of the emission intensities, and supersonic-jet experiments can provide information on the excited states of cooled and collision-free molecules. However, it is generally difficult to obtain the highly resolved phosphorescence spectra in a jet. With molecules that exhibit a prominent temperature dependence of the emission spectra, we can obtain information on the excited- and ground-sate populations through the temperature dependence of the emission and excitation spectra.

In the present work, emission and excitation spectra of isophthalaldehyde vapor have been measured at different temperatures in the presence of an added buffer gas. The mission is shown to consist of the $T_1(n, \pi^*) \rightarrow S_0$ phosphorescence accompanied by the weak thermally activated $S_1(n, \pi^*) \rightarrow S_0$ delayed fluorescence, just as the case of benzaldehyde vapor.[8,9]
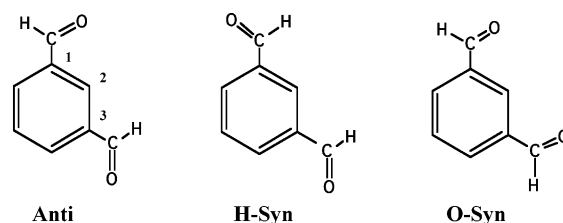
Isophthalaldehyde (Benzene-1,3-dicarboxaldehyde)

Figure 1. Molecular structures of the three stable rotamers of isophthalaldehyde (IP).

The $S_1−T_1$ energy separations obtained from the temperature dependence of the emission spectra agreed well with those obtained from the spectral band locations. The temperature dependence of the multiple peaks observed in the main phosphorescence and excitation bands in highly resolved spectra provides the energy differences among the three rotational isomers in the S_0, S_1, and T_1 states, which are in good agreement with those obtained by DFT calculations. It is demonstrated that the first, second, and third peaks in the main phosphorescence bands belong to the anti (O-trans), H-syn (H-cis), and O-syn (O-cis) rotational isomers, respectively, whereas the corresponding peaks in the excitation origin belong to the anti, O-syn, and H-syn rotational isomers, respectively.

2. Experimantal and Computational Methods

Isophthalaldehyde (IP) obtained from Aldrich, was purified by means of repeated recrystallizations in hexane. White needle crystals with the melting point of 90 °C were obtained. Perfluorohexane obtained from Aldrich, was used as a buffer gas. The absence of any impurity emission in glassy matrix at 77 K and verification that the phosphorescence excitation spectra in the vapor phase agreed well with the absorption spectra suggest that the purified samples were sufficiently pure for the experiment. The samples were degassed in an all-glass made vacuum system equipped with a diffusion pump. Details of the sample preparation are described in a foregoing paper.[11] The

* Corresponding author. E_mail: titoh@hiroshima-u.ac.jp.

sample and buffer gas pressure were always kept below the saturation pressures at the temperatures employed in the present study. Because IP vapor was found to be unstable with respect to photon irradiation and to degrade during long-time scanning, all the measurements were carried out only once for each fresh sample just after the preparation. During the measurement, the temperature of the sample cell was controlled by a thermostated cell holder that consists of the lower and upper parts. The lower part covers most of the quartz square cell for which the emission is detected. The temperature of the upper part of the cell was kept slightly lower than that of the lower part. For most of the emission measurements square 10 mm path length quartz cells were used.

UV−vis absorption spectra were measured with a Shimadzu UV-2550 spectrophotometer, and the emission and excitation spectra were measured with a Spex Fluorolog-3 (Model 21-SS) spectrophotometer. The latter photometer, designed especially for the measurements of weak emission signals, is equipped with a double-grating excitation monochromator, a high-pressure 450 W Xenon lamp as an excitation-light source and a photomultiplier tube (Hamamatsu R928-P) in an electric-cooled housing operated in photon-counting mode to detect weak signals. With this apparatus the signal from an emitting entity expressed by the product of the emission quantum yield and the optical density being as low as 10^{-7}, can be measured with a reasonable S/N ratio. In most of the emission and excitation measurements, the silt width was kept near 2.0 Å (8.0 cm^{-1} at 500 nm). Wavelength calibration of the spectrophotometer was carried out using a Melles Griot He−Ne green laser (5435 Å). Infrared absorption spectra were measured with a JASCO IR-810 spectrophotometer.

In the present experiment a buffer gas was added to the sample vapor, because the emission of the samples is weak without the buffer gas and addition of the buffer gas induces sufficient collisional relaxation. The samples were found to be unstable with respect to the photon irradiation and to degrade during long-time measurements. In the course of the experiment, IP vapor was found to degrade to form benzaldehyde, presumably through the decomposition reaction, $C_6H_4(CHO)_2 \rightarrow C_6H_5$-$CHO + CO$ in case no buffer gas was added. It is known that at low pressure benzaldehyde vapor decomposes to form benzene and carbon monoxide upon the UV irradiation into the $S_2 (\pi, \pi^*)$ state.[12]

Quantum chemical calculations were carried out not only with the density-functional theory (DFT) but also with semiempirical SCF-MO methods at MNDO, AM1, and PM3 levels. The DFT calculations were carried out using the GAUSSIAN 03 program.[13] Optimized geometries, total energies of the ground-state molecules and harmonic wavenumbers were obtained by DFT calculations using the 6-311++G(3df,2pd) basis set. Becke's three-parameter exchange functional has been used for the DFT calculations,[14] together with the correlation functionals of Lee−Yang−Parr (B3LYP).[15]

3. Results and Discussion

3.1. UV−Vis and Infrared Absorption Spectra and Emission Spectrum in the Condensed Phases. The UV−vis and infrared absorption spectra and the emission spectrum of IP in the condensed phases are first described briefly, because only a little information is available for the spectroscopy of this molecule in the literature. Figure 2 shows the absorption spectrum in hexane at room temperature and emission and excitation spectra in a methylcyclohexane−isopentane (1:1) mixture at 77 K. The comparatively strong absorption band at
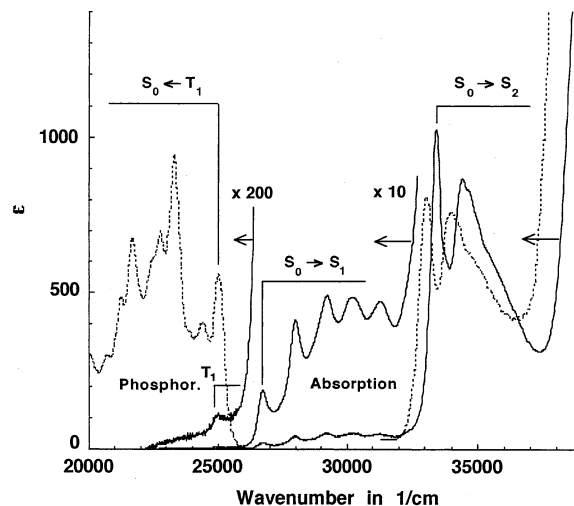

Figure 2. Absorption spectrum in hexane at room temperature (solid-line spectrum), phosphorescence and corrected excitation spectra (dotted-line spectra) in an isopentane−methylcyclohexane (1:1) mixture at 77 K of low concentration IP.

33 500 cm^{-1} is due to the $S_0 \rightarrow S_2(\pi, \pi^*)$ transition. The absorption spectra at wavenumbers below 32 000 cm^{-1} consist of the weak bands located at about 25 000 cm^{-1} and the structured ones starting from 26 700 cm^{-1}. In light of the molar extinction coefficients and the band locations, the former weak bands are attributed to the $S_0 \rightarrow T_1(n, \pi^*)$ transition and the latter to the $S_0 \rightarrow S_1(n, \pi^*)$ transition. The emission spectrum at 77 K shows the characteristic feature of the C=O stretching vibration with the frequency of about 1700 cm^{-1}, and the apparent emission origin at 25 000 cm^{-1} agrees well with the $S_0 \rightarrow T_1$ absorption origin in hexane at room temperature. Further, the excitation spectrum of the emission corresponds well to the absorption spectrum. It follows from these observations that the emission is safely assigned to the phosphorescence from $T_1(n, \pi^*)$. Thus, the emission and absorption spectral features of IP are similar to those of benzaldehyde or its derivatives.[8−10] We could not find any evidence indicating the presence of the different rotamers neither in the absorption nor in the emission spectra in the condensed phases.

Figure 3 shows the infrared absorption spectrum of IP in a 900−1800 cm^{-1} region along with the spectra obtained by the DFT calculation. Because the absorption bands of carbon tetrachloride used as the solvent and those of IP overlap in part with each other, only the infrared bands of IP were extracted. The calculated spectra demonstrate that the band location and intensity differ subtly depending on the rotamer. There is good agreement between the calculated and observed spectra, although the observed spectrum consists of those of the mixture of the three rotational isomers contained in a certain ratio. The band in the characteristic C=O stretching region shows a sort of multiple band feature. The comparison of the measured and calculated infrared spectra shows clearly the coexistence of the three rotamers. A simple simulation based on the superposition of the calculated spectra demonstrates that the anti, H-syn, and O-syn rotamers coexist in a population ratio of approximately 10:8:3 for IP in carbon tetrachloride at 20 °C.

3.2. Absorption, Emission, and Excitation Spectra in the Vapor Phase. Figure 4 shows the emission spectra of IP vapor at different temperatures in the presence of 290 Torr perfluorohexane. These spectra exhibit a prominent temperature dependence: The intensity of the weak band at near 26 700 cm^{-1} relative to the strong band at near 25 000 cm^{-1} increases significantly with increasing temperature. Further, the former

Rotational Isomers of Isophthalaldehyde Vapor

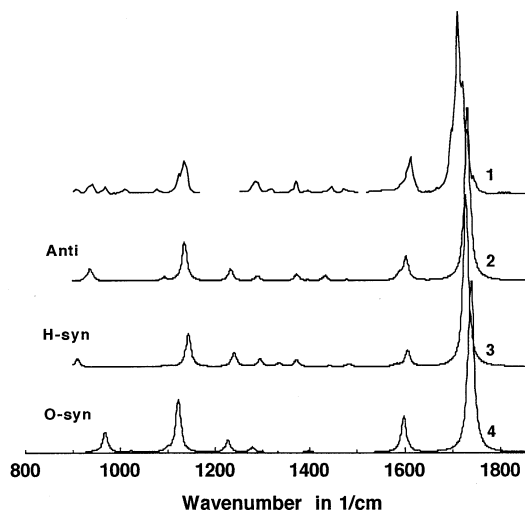*J. Phys. Chem. A, Vol. 111, No. 34, 2007* **8441**

Figure 3. Measured (1) and calculated (2−4) infrared absorption spectra of IP. Spectrum 1 is obtained in carbon tetrachloride at 20 °C. The intensities, I_0, and locations, ν_0, in the calculated spectra are obtained from the results of the DFT calculation and the spectral profiles are modified by Lorentzians, $I = I_0/[(\nu - \nu_0)^2 + b^2]$, to fit the band shape of the observed spectrum by varying b.
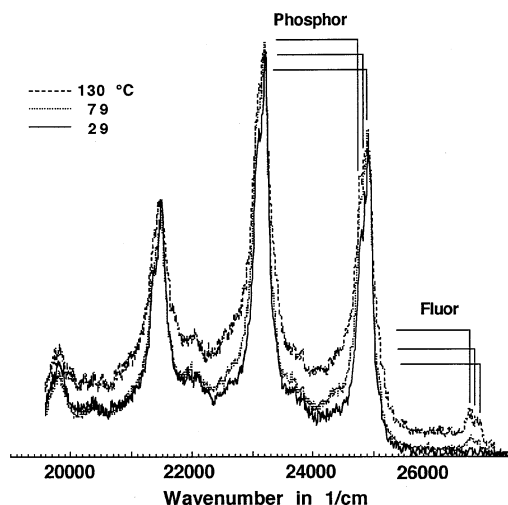

Figure 4. Emission spectra of IP vapor in the presence of 290 Torr perfluorohexane at different temperatures.

and latter emission bands correspond well to the $S_0 \rightarrow S_1(n, \pi^*)$ and the $S_0 \rightarrow T_1(n, \pi^*)$ excitation origins, respectively, as shown in Figure 5. These spectral features are almost the same as those of the $T_1(n, \pi^*)$ phosphorescence and thermally activated $S_1(n, \pi^*)$ delayed fluorescence observed for benzaldehyde vapor.[8] Thus, the emission peak at near 26 700 and 25 000 cm^{-1} can be assigned, respectively, to the $S_1(n, \pi^*)$ delayed fluorescence and $T_1(n, \pi^*)$ phosphorescence origin bands.

To confirm the present assignment, the relative emission intensities have been analyzed quantitatively. When two closely located electronic states are in thermodynamic equilibrium, the quantum yield ratio of the emission from the lower state (T_1) to that from the upper state (S_1), Φ_P/Φ_F, is given approximately by, $\Phi_P/\Phi_F = (k_P/k_F) \exp[\Delta E_{S-T}/kT]$, where ΔE_{S-T} is the S_1-T_1 energy separation, k_F and k_P are respectively the radiative rate constants of the S_1 and T_1 states, and T is the absolute temperature. We have used the integrated intensities of the fluorescence and phosphorescence origin bands subtracted by the background intensities, I_F and I_P, respectively, instead of Φ_F and Φ_P. The temperature dependence of I_P/I_F is shown in
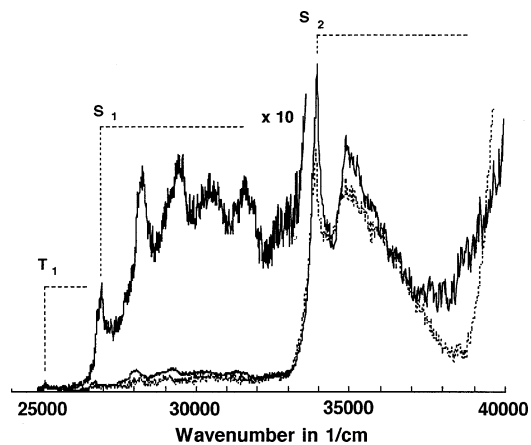

Figure 5. Absorption (solid line) and corrected excitation (dotted line) spectra of IP vapor. The excitation spectrum was obtained in the presence of 290 Torr perfluorohexane.
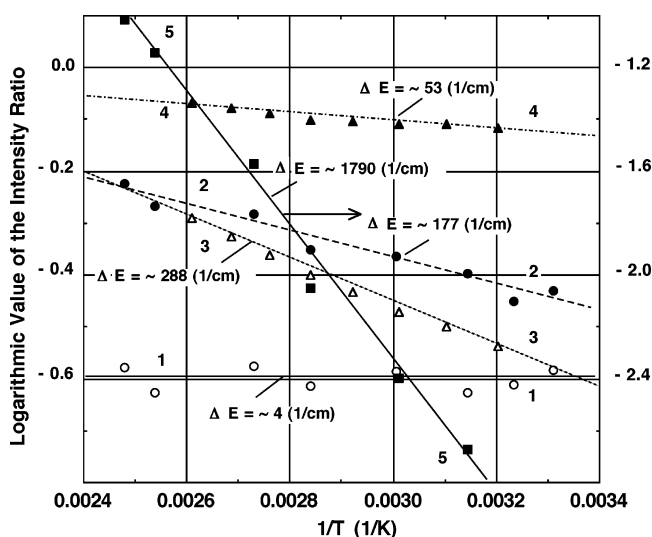

Figure 6. Logarithmic values of the band intensity ratios plotted against the reciprocal of the absolute temperature: (1) P_2/P_1; (2) P_3/P_1; (3) F_2/F_1; (4) F_3/F_1; (5) I_P/I_F (fluorescence/phosphorescence).

Figure 6. The ΔE_{S-T} and k_P/k_F values obtained from the logarithmic values of I_P/I_F plotted against $1/T$ are 1790 ± 80 cm^{-1} and 0.006, respectively. If we take the S_1 fluorescence peak at 26 745 cm^{-1} and T_1 phosphorescence peak at 24 940 cm^{-1} as the S_1 and T_1 origins, respectively, then the ΔE_{S-T} value of IP vapor is evaluated to be 1805 cm^{-1}. This value agrees well with that estimated from the temperature dependence of the emission spectrum. The obtained k_P/k_F values are also in reasonable agreement with the $S_0 \rightarrow T_1/S_0 \rightarrow S_1$ origin-band intensity ratio seen in the absorption spectrum in hexane (about 0.01). The spectral analysis mentioned here is based on a crude treatment, as will be described in detail later. As seen in Figure 4, multiple peaks are observed in the phosphorescence, fluorescence, and excitation main bands. These bands are shown to be originating from the different rotamers in the next section.

3.3. Spectral Assignments and the Energy Levels of the Three Rotational Isomers in the Vapor Phase. Figure 7 shows the emission and excitation spectra in an expanded scale for IP vapor in the presence of 290 Torr perfluorohexane. As mentioned, the observed emission consists of the weak delayed fluorescence from $S_1(n, \pi^*)$ and the strong phosphorescence from $T_1(n, \pi^*)$, showing a characteristic progression in the C=O stretching vibration. Closer inspection of the spectra reveals the appearance of the three peaks in the phosphorescence and
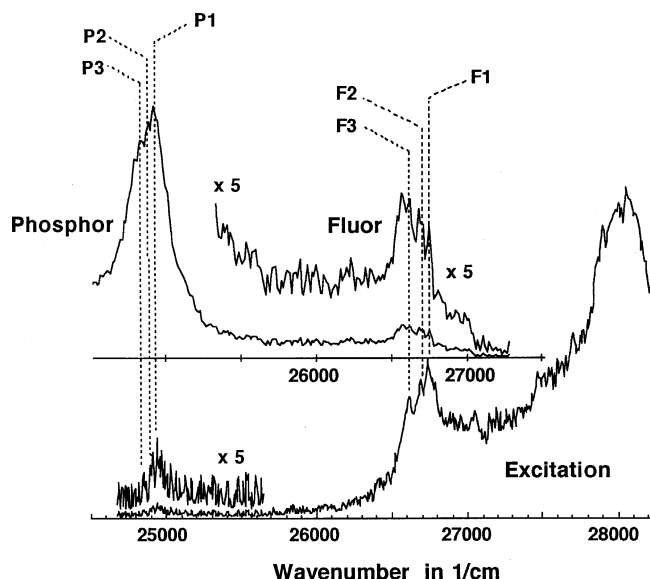
Figure 7. Excitation and emission spectra of IP vapor in the presence of perfluorohexane in an expanded scale.

the $S_0 \rightarrow S_1(n, \pi^*)$ excitation origins. The strongest phosphorescence peak, P_1, at 24 940 cm^{-1} agrees in position with the apparent $S_0 \rightarrow T_1(n, \pi^*)$ excitation origin. It is also seen vaguely in Figure 7 that the phosphorescence peaks, P_2 and P_3, correspond to the weak excitation peaks located at energies slightly lower than the main excitation peak. Further, the three fluorescence peaks, F_1(26 745 cm^{-1}), F_2(26 680 cm^{-1}), and F_3-(26 615 cm^{-1}) in the fluorescence origin correspond to the three peaks in the $S_0 \rightarrow S_1$ excitation origin region. The similar multiple peaks are observed also in the second excitation band near 28 000 cm^{-1}.

The characteristic multiple peaks observed in the $T_1(n, \pi^*)$ $\rightarrow S_0$ phosphorescence and the $S_0 \rightarrow S_1(n, \pi^*)$ excitation origin bands of IP vapor are assigned to those originating from the three different rotamers on the basis of the following observations: (1) Such a characteristic multiple structure is not observed in the phosphorescence and excitation spectra of other aromatic carbonyl compound vapors for which no stable rotamer exists. (2) The intensities of the lower-energy peaks in the main phosphorescence origin bands are too high to assign them as the combinations with the C=O stretching mode or sequence bands. (3) There are no vibrational modes with frequency below 80 cm^{-1} in the calculated vibrational frequencies in the ground state of IP. (4) The observed temperature dependence of the emission and excitation spectra as well as the band locations can be explained reasonably, if we assign the three peaks in the main phosphorescence and the first excitation bands as those originating from the three different rotamers. This is discussed below in detail.

Figure 8a shows the phosphorescence spectra in the origin band region measured at different temperatures. One can see that the relative intensity of the phosphorescence peak P_3 at 24 805 cm^{-1} increases with increasing the temperature. To determine the relative band intensities at different temperatures, the main phosphorescence bands were simulated by sum of Lorenztians, $\Sigma_i I(\nu_i)/[(\nu - \nu_i)^2 + c\Delta B_i^2]$, where the parameters c and $I(\nu_i)$, were adjusted to fit the observed spectral patterns measured at different temperatures. The bandwidths, ΔB_i, of the main phosphorescence bands are also found to change with the temperature. In the case of the first phosphorescence band, the ΔB_i value changes from 250 to 330 cm^{-1} with increasing the temperature from 20 to 130 °C. Because the bandwidth
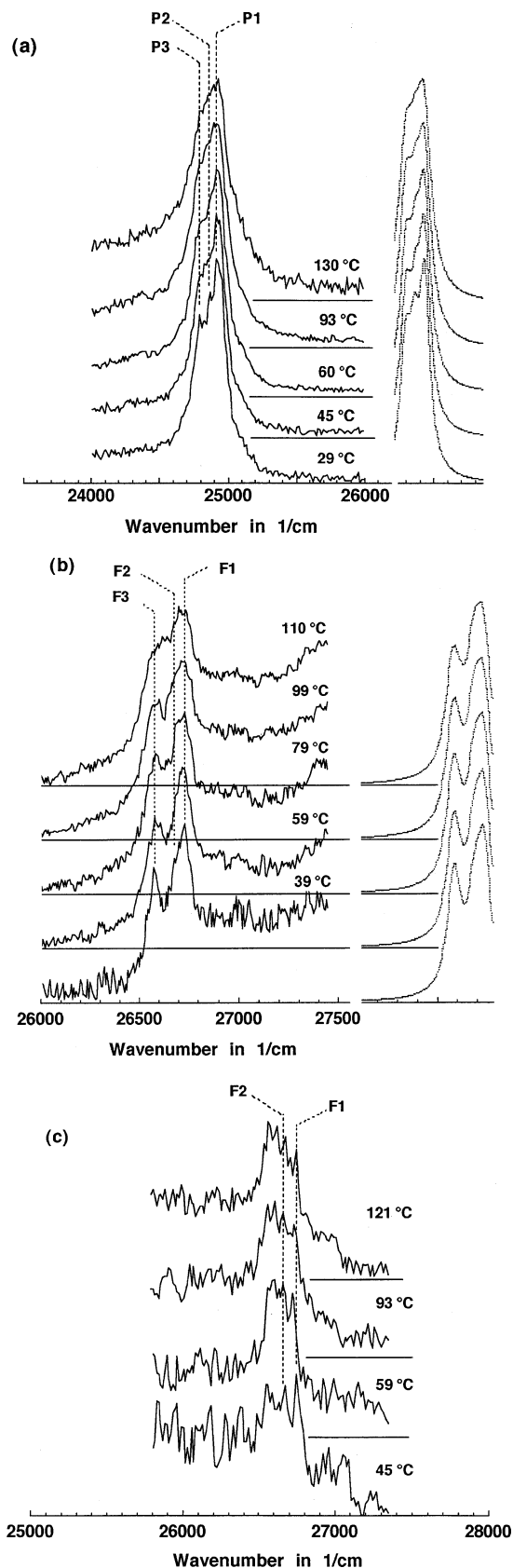

Figure 8. (a) Observed and calculated phosphorescence spectra of IP vapor at different temperatures in an expanded scale. (b) Observed and calculated excitation spectra of IP vapor at different temperatures in an expanded scale. (c) Observed delayed fluorescence spectra of IP vapor at different temperatures in an expanded scale.

influences the estimation of the band intensities, the half-value widths, $\Delta B_{1/2}$, of the main bands were obtained by varying the

Rotational Isomers of Isophthalaldehyde Vapor

J. Phys. Chem. A, Vol. 111, No. 34, 2007 **8443**

slit width of the detection monochromator from 1.8 to 3.5 Å and by extrapolating it to 0 Å. The $\Delta B_{1/2}$ values thus obtained are found to be fit well by an exponential function of the absolute temperature (T), $\Delta B_{1/2} = B_0 \exp(0.0027T)$, with the correlation coefficient of 0.96. The B_0 value extrapolated to $T = 0$ K is found to be 112 cm⁻¹. Thus, the relation $\Delta B_i = 112 \exp(0.0027T)$ cm⁻¹ was used for the simulation. The results of the simulations are shown also in Figure 8a. Although the observed phosphorescence spectrum contains spectral congestion arising from the combination bands with the C=O stretching mode and the hot bands, the temperature dependence of the phosphorescence spectrum is reproduced reasonably by the simulated spectra. Using the integrated intensities of the Lorenztians, the logarithmic values of the peak intensity ratios, $I(P_2)/I(P_1)$ and $I(P_3)/I(P_1)$, are plotted against $1/T$ (Figure 6). The energy differences obtained from the two slopes of the plots in Figure 6 are found to be 4 ± 20 cm⁻¹ for the ratio $I(P_2)/I(P_1)$ and 177 ± 20 cm⁻¹ for $I(P_3)/I(P_1)$ ($\ln(I_1/I_2) = -\Delta E_{12}/kT$ + constant). Because the three peaks in the phosphorescence origin region are separated by 55 cm⁻¹ for P_1-P_2 and 135 cm⁻¹ for P_1-P_3, the energy differences between the two rotamers in the ground state are evaluated to be 59 ± 20 cm⁻¹ (=(55 + 4) $\pm$ 20 cm⁻¹) and 312 ± 20 cm⁻¹ (=(135 + 177) $\pm$ 20 cm⁻¹). The results of the DFT calculation show that the anti rotamer is lower in energy than the H-syn and O-syn rotamers, respectively, by 25.2 and 309.0 cm⁻¹ for IP in the ground state. This situation is supported also by the semiempirical SCF-MO calculations, although the calculated anti−O-syn energy differences in the ground state are somewhat small: 57.3 cm⁻¹ for anti−H-syn and 230.7 cm⁻¹ for anti−O-syn with AM1, 23.1 cm⁻¹ for anti−H-syn and 173.2 cm⁻¹ for anti−O-syn with MNDO, and 63.8 cm⁻¹ for anti−H-syn and 190.2 cm⁻¹ for anti−O-syn with PM3 calculation. Hence, the P_1, P_2, and P_3 peaks in the phosphorescence origin region are assigned, respectively, to those of the anti, H-syn, and O-syn rotamers. Assignments of the peaks observed in the emission spectrum of IP vapor are summarized in Table 1, where the bands for the three rotamers (anti, H-syn, and O-syn) are indicated. These assignments were carried out in light of the observed and calculated infrared data as well as the results of the DFT calculation. The fundamental frequencies of the C=O stretching mode in the phosphorescence spectra are found to be 1725 cm⁻¹ for the anti and H-syn rotamers and 1730 cm⁻¹ for the O-syn rotamer.[19] The interval between the strong C=O stretching bands of the anti and O-syn rotamers, therefore, tends to separate from 135 to 140 cm⁻¹ and from 140 to 145 cm⁻¹, respectively, on the vibrational quantum number going from 0 to 1 and from 1 to 2, which is what is actually observed (Table 1). Actually, there are two C=O stretching modes, symmetric and antisymmetric, with the DFT-calculated frequencies of 1730.6 and 1729.1 cm⁻¹ for the anti, 1734.2 and 1726.5 cm⁻¹ for the H-syn, and 1738.4 and 1731.1 cm⁻¹ for the O-syn rotamer, respectively. In the infrared spectra, the antisymmetric C=O mode appears predominantly for the H-syn rotamer, and both the symmetric and antisymmetric C=O modes appear for the anti and O-syn rotamers. The calculated frequency of the symmetric C=O stretching mode of the O-syn rotamer also is somewhat high as compared with those of the anti and H-syn rotamers.

The intensity of the excitation spectrum reflects the relative populations of the closely located levels in the ground state. Therefore, we can observe directly the temperature dependence of the population in the ground state by measuring the excitation spectra at different temperatures. Figure 8b shows the excitation spectra of IP vapor near the $S_0 \rightarrow S_1(n, \pi^*)$ origin measured at

TABLE 1: Locations and the Assignments of the Bands Observed in the Emission Spectrum of IP Vapor.

ν (cm⁻¹),[a] intensity[b]	assignment[c]	infrared (cm⁻¹)[d−f]	
26745, w	S_1(0−0) anti		
26680, w	S_1(0−0) O-syn		
26615, w	S_1(0−0) H-syn		
24940, vs	T_1(0−0) anti		
24885, vs	T_1(0−0) H-syn		
24805, vs	T_1(0−0) O-syn		
23810, w	1135 anti	1132[e]	1134.8[d]
23680, w	1125 O-syn	1120[e]	1121.7[d]
23215, vs	1725 anti	1722[e]	1730.6[d] (sym C=O)[f]
23165, vs	1725 H-syn	1722[e] (antisym C=O)[f]	1734.2[d] (sym C=O)[f]
23075, vs	1730 O-syn	1727[e] (sym C=O)[f]	1738.4[d] (sym C=O)[f]
22080, w	1725 + 1135 anti		
21950, w	1730 + 1125 O-syn		
21510, s	1725 × 2 anti		
21460, s	1725 × 2 H-syn		
21365, s	1730 × 2 O-syn		
19825, m	1725 × 3 anti		

[a] The band locations have been determined with an accuracy of ±5 cm⁻¹. [b] Key: w, weak; m, medium; s, strong; vs, very strong. [c] The vibrational frequencies in the ground state are indicated. [d] Obtained by the DFT calculations, with the modification that the harmonic wavenumbers ν_{harm} were scaled by $\nu_{calc} = \nu_{harm} \times (0.9727 + 0.00000201 \times \nu_{harm})$ to reproduce the observed spectra. [e] Infrared band locations in Ar matrix at 15 K (Ohno, K.; Itoh, T. *J. Phys. Chem. A*, in press).[16] [f] sym C=O: symmetric C=O stretching mode. antisym C=O: antisymmetric C=O stretching mode.

different temperatures. It is seen that the relative intensity of the lower-energy peak F_3 (26 630 cm⁻¹) increases with increasing the temperature. To determine the relative band intensities, the excitation spectra were simulated by the sum of Lorenztians in the way already mentioned. The result of the simulation is shown also in Figure 8b, where the temperature dependence of the observed spectra is reproduced reasonably. The energy differences of 53 ± 10 and 288 ± 10 cm⁻¹ are obtained, respectively, from the logarithmic values of the intensity ratios $I(F_2)/I(F_1)$ and $I(F_3)/I(F_1)$ plotted against $1/T$ (see Figure 6). Considering the errors introduced in evaluation of the relative intensities, these energy differences agree surprisingly well not only with those obtained from the phosphorescence data but also with the DFT outputs.

A similar analysis might be possible for the temperature dependence of the fluorescence spectra, but this could not be carried out because of the poor S/N ratio of the weak fluorescence spectra. However, one can see vaguely in Figure 8c that the intensity of the second fluorescence band F_2 (O-syn) relative to that of the first band F_1 (anti) increases with increasing the temperature. This observation demonstrated also that the S_1 level of the O-syn rotamer is located at energies higher than that of the anti rotamer.

In Figure 9, we show the energy diagrams obtained in the present work for the excited and ground states of the three rotamers of IP vapor. The ground states of the H-syn and O-syn rotamers are located at energies higher than that of the anti rotamer, respectively, by about 50 and 300 cm⁻¹. The energy difference between the anti and O-syn rotamers in the $S_1(n, \pi^*)$ state is estimated to be about 240 cm⁻¹ and the S_1 level of the H-syn rotamer is located at energies slightly lower than that of the anti rotamer. The $T_1(n, \pi^*)$ states of the anti and H-syn rotamers are almost isoenergetic to each other and the T_1 state of the O-syn rotamer is located at energies about 170 cm⁻¹
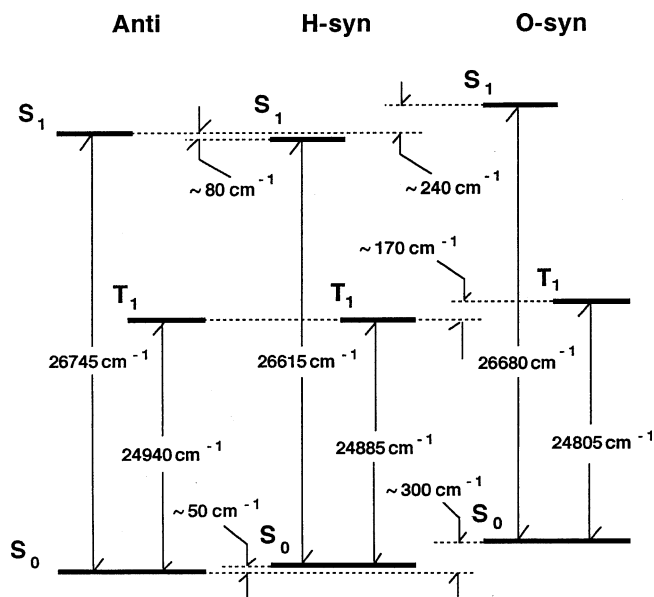
Figure 9. Ground- and excited-state energy levels of the three rotamers of IP obtained spectroscopically.

higher than that of the anti rotamer. The O-syn:H-syn:anti population ratio in the ground state at 20 °C deduced from the anti−H-syn and anti−O-syn energy differences is 0.23:0.78: 1.0. Interestingly, this ratio is almost in agreement with that obtained from the infrared data measured in carbon tetrachloride at 20 °C (0.3:0.8:1.0), although the environmental situations are different between the vapor and solution phases.

4. Conclusions

The mission of IP vapor is shown to consist of the $T_1(n, \pi^*)$ → S_0 phosphorescence accompanied by the weak thermally activated $S_1(n, \pi^*)$ → S_0 delayed fluorescence. The S_1–T_1 energy separations obtained from the temperature dependence of the emission spectra agreed well with those obtained from the band locations. The peaks corresponding to the three rotamers, anti, H-syn, and 0-syn, were identified in the emission and excitation spectra. Most of the observed main emission bands were reasonably assigned by considering the three rotamers. The temperature dependence of the relative intensity of the phosphorescence and excitation spectra of IP vapor provides anti−O-syn energy differences of about 300 cm^{-1} in the ground state, 180 cm^{-1} in the T_1 state, and 240 cm^{-1} in the S_1 state, and anti−H-syn energy differences of about 50 cm^{-1}

in the ground state, almost 0 cm^{-1} in the T_1 state, and 80 cm^{-1} in the S_1 state. The energy differences in the ground state are in reasonable agreement with the DFT outputs. IP is considered to be one of the rare examples for which the three stable rotamers were identified in the emission and excitation spectra, and for which the energy levels of the three rotamers were determined in the ground, excited singlet, and excited triplet states.

References and Notes

(1) Itoh, T. *J. Phys. Chem. A* **2006**, *110*, 10012.
(2) Casarini, D.; Lunazzi, L.; Mazzanti, A. *J. Org. Chem.* **1997**, *62*, 7592.
(3) Schaefer, T.; Penner, G. H.; Sebastian, R.; Takeuchi, C. S. *Can. J. Chem.* **1986**, *64*, 158.
(4) Bernassau, J. M.; Drakenberg, T.; Liljefors, T. *Acta Chem. Scand.* **1977**, *B31*, 836.
(5) Gebicki, J.; Kuberski, S. *J. Chem. Soc., Chem. Commun.* **1988**, 1364.
(6) Lal, B. B.; Srivastava, M. P.; Singh, I. S. *Ind. J. Pure Appl. Phys.* **1971**, *9*, 857.
(7) Srivastava, M. P.; Lal, B. B.; Singh, I. S. *Ind. J. Pure Appl. Phys.* **1972**, *10*, 570.
(8) Stockburger, M. *Z. Phys. Chem.* **1962**, *31*, 350.
(9) Itoh, T.; Baba, H.; Takemura, T. *Bull. Chem. Soc. Jpn.* **1978**, *51*, 2841.
(10) Itoh, T. *J. Mol. Struct.* **2004**, *705*, 113.
(11) Itoh, T. *Spectrochim. Acta A* **2002**, *59A*, 61.
(12) Berger, M.; Goldblatt, I. L.; Steel, C. *J. Am. Chem. Soc.* **1973**, *95*, 1717.
(13) Frisch, M. J.; Trucks, G. W.; Schlegel, H. B.; Scuseria, G. E.; Robb, M. A.; Cheeseman, J. R.; Montgomery, J. A.; Vreven, T., Jr.; Kudin, K. N.; Burant, J. C.; Millam, J. M.; Iyengar, S. S.; Tomasi, J.; Barone, V.; Mennucci, B.; Cossi, M.; Scalmani, G.; Rega, N.; Petersson, G. A.; Nakatsuji, H.; Hada, M.; Ehara, M.; Toyota, K.; Fukuda, R.; Hasegawa, J.; Ishida, M.; Nakajima, T.; Honda, Y.; Kitao, O.; Nakai, H.; Klene, M.; Li, X.; Knox, J. E.; Hratchian, H. P.; Cross, J. B.; Adamo, C.; Jaramillo, J.; Gomperts, R.; Stratmann, R. E.; Yazyev, O.; Austin, A. J.; Cammi, R.; Pomelli, C.; Ochterski, J. W.: Ayala, P. Y.; Morokuma, K.; Voth, G. A.; Salvador, P.; Dannenberg, J. J.; Zakrzewski, V. G.; Dapprich, S.; Daniels, A. D.; Strain, M. C.; Farkas, O.; Malick, D. K.; Rabuck, A. D.; Raghavachari, K.; Foresman, J. B.; Ortiz, J. V.; Cui, Q.; Baboul, A. G.; Clifford, S.; Cioslowski, J.; Stefanov B. B.; Liu, G.; Liashenko, A.; Piskorz, P.; Komaromi, I.; Martin, R. L.; Fox, D. J.; Keith, T.; Al-Laham, M. A.; Peng, C. Y.; Nanayakkara, A.; Challacombe, M.; Gill, P. M. W.; Johnson, B.; Chen, W.; Wong, M. W.; Gonzalez, C.; Pople, J. A. *Gaussian 03*, revision B.05; Gaussian, Inc.: Pittsburgh, PA, 2003.
(14) Becke, A. D. *J. Chem. Phys.* **1993**, *98*, 5648.
(15) Lee, C.; Yang, W.; Parr, R. G. *Phys. Rev. B* **1988**, *37*, 785.
(16) Ohno K.; Itoh, T. *J. Phys. Chem. A,* in press.